Resonant nanophotonic spectrum splitting for ultra-thin multijunction solar cells

Supporting information

Sander A. Mann, Erik C. Garnett

Center for Nanophotonics
FOM institute AMOLF
garnett@amolf.nl

Contents

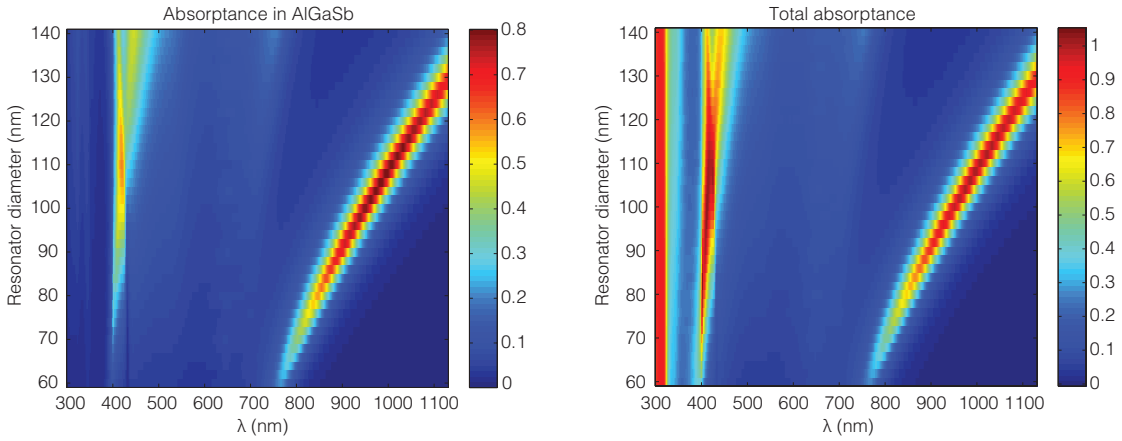

Figure S1: Absorptance as a function of diameter and wavelength in the semiconductor (left) and in the total structure (right).

1 Full absorption spectra

To calculate the short circuit current we integrated the absorption from 300 nm to the band gap of the material. Hence, in this section we show those full absorption spectra of all the simulations that are used in the main text.

In Fig. S1 the absorption spectra are shown for the array comprising a single resonator. On the left hand the absorptance in the semiconductor is shown, while on the right side the absorption in the total array is shown. Note that the absorption in the total array, calculated as $1-R$ where R is the reflection, goes slightly over one (to 1.02) at around 400 nm. This is due to a very strong grating resonance, and convergence studies show that this result can be reduced closer to one. However, this does not affect our results because the simulation is converged at all other wavelengths and the integrated absorption thus does not change noticeably.

The absorption remains strong right up to the band gap because the reported refractive index has few data points near the band gap (0.1 eV spacing), so we used the band gap reported in [1] as a hard cut off. A change in band gap only affects absolute numbers, and since we're mostly interested in relative enhancements this does not change the conclusions of this Letter. More information on the refractive indices used and simulation set-up is given in section 4 of this supplementary information.

Fig. S2 shows the full absorption spectra corresponding to Fig. 3 in the main text. Because in this case the array is no longer rotation symmetric, there are two polarizations that are described by the axis shown in the cartoon in Fig. 3a. As shown below the

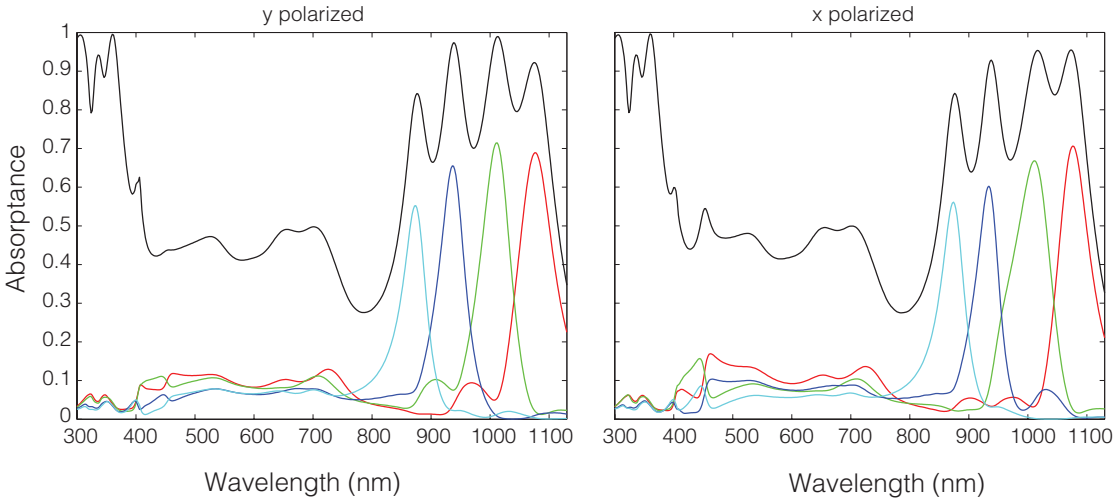

Figure S2: Absorption over the full solar range for the AlGaSb resonator array, with the electric field polarized along the y (left) and x (right) directions, as shown in the schematic in Fig. 4a in the main text.

spectra are slightly different, which is due to the difference between “closest particle" when the polarization is changed. For example, the 98 nm resonator (absorption in blue) seems to be affected more by the 110 nm resonator (absorption in green) when the polarization is perpendicular to the spacing in between them.

Similarly we have the full absorption spectrum for the multijunction array described in Fig. 4 in the main text, as shown in Fig. S3.

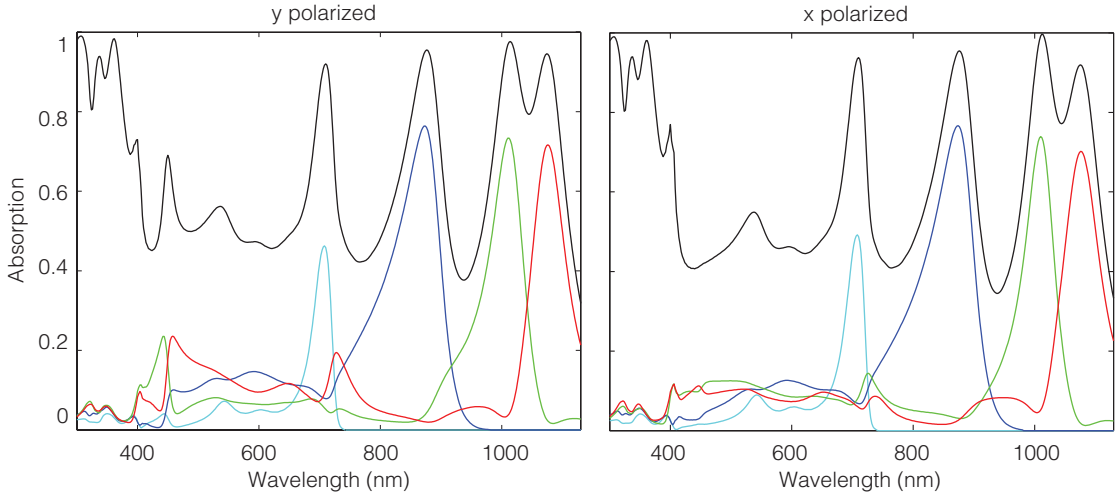

Figure S3: Absorption over the full solar range for the multijunction resonator array, with the electric field polarized along the y (left) and x (right) directions, as shown in the schematic in Fig. 5a in the main text.

2 Angle dependence of absorption

To probe the angular response of our array we used S4 [2], because of its convenience for angular investigations. The absorption of an array of AlGaSb particles as a function of angle is shown in Fig. S4 for s and p polarizations. This particular array had two resonators with 84 nm diameter, one with 104 nm diameter and one with 124 nm diameter. The degenerate pair leads to full absorption at 780 nm, where a single resonator would not achieve this (see Fig. S1 in this supporting information).

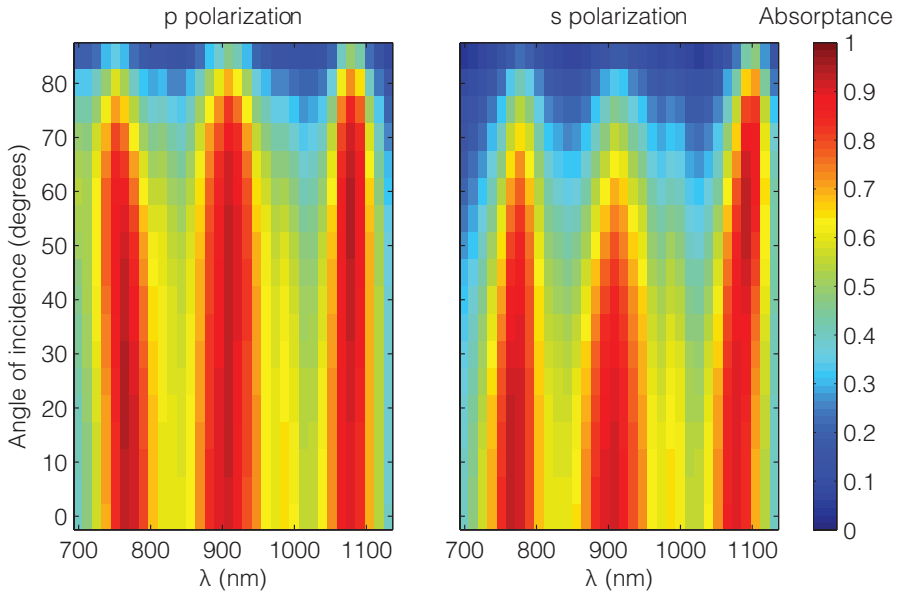

Figure S4: Absorption as a function of angle for s and p polarized light for an array with two 84 nm, one 104 and one 124 nm diameter resonators in the unit cell.

Clearly the absorption only starts to deviate at angles larger than 80 degrees, which is consistent with literature reports on MIM resonators. [3] Calculating the difference in recombination rate using Eq. 3b in the main text we find that due to the increased reflection of the array at large angles the recombination rate in fact is reduced compared to a truly isotropic absorption spectrum, but only by 2.5%. Since the V_{oc} goes with the natural logarithm of the ratio of generation over recombination rate, this small decrease barely affects the results and can thus safely be ignored.

3 Efficiency of a single resonator periodic device

For completeness below the efficiency and short circuit current are shown together with the same V_{oc} plot shown in the main text in figure 3. Clearly, although the voltage shows significant shifts, the efficiency is still dominated by the current. The plateau between 90-100 nm diameter is due to shifting of the resonance over an atmospheric absorption band in the solar spectrum.

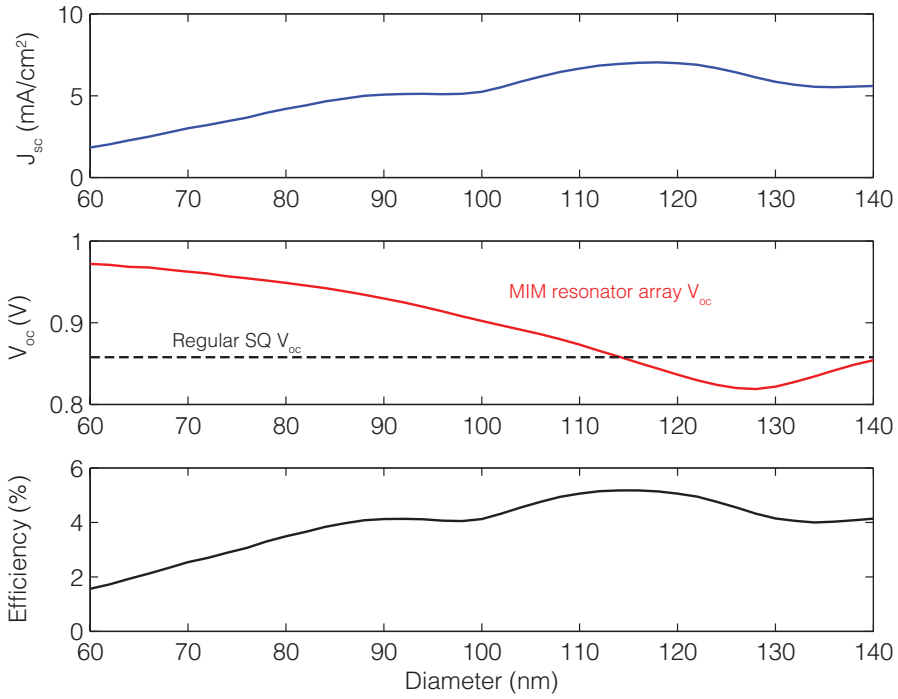

Figure S5: Short circuit current (top panel), voltage (middle panel), and efficiency (bottom panel) for different resonator diameters for the array with a single resonator, shown in Fig. 2 in the main text.

4 Simulation details

All numerical simulations aside from the angle scan shown in Fig. S4 are done with Lumerical FDTD. A schematic of the simulation set-up is shown below. The absorption in the semiconductor material is calculated based on a power flow box, such that the net power flow into the box can be calculated, which is equal to the absorption. To avoid interface issues the horizontal monitors are situated 0.5 nm away from the semiconductor-metal interface, so technically not all absorbed power is collected, but we assume that only a small fraction of the total absorption occurs within that 0.5 nm. In any case, any absorption that is missed leads to an underestimation of the current and thus efficiency.

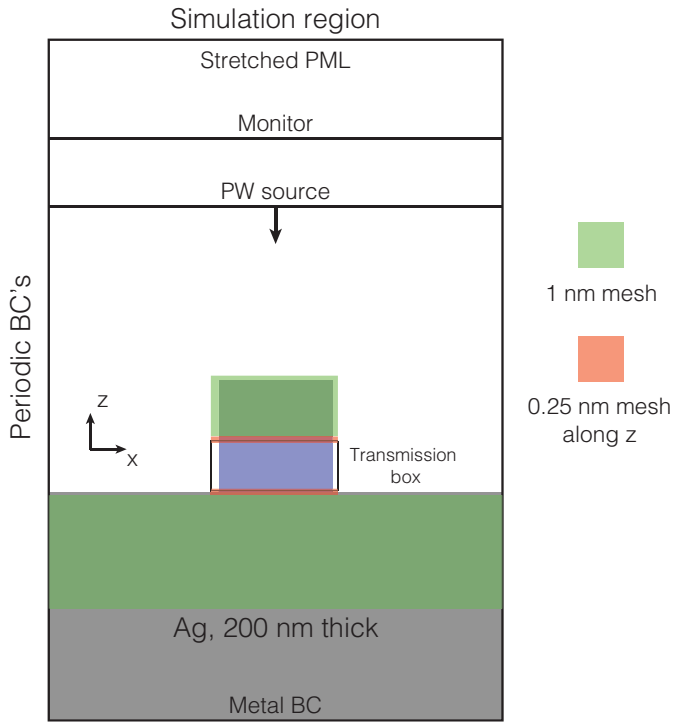

Figure S6: Set-up of the FDTD simulation. The green and orange shaded areas refer to refinement meshes, BC stands for boundary condition.

The dielectric constants we have used for AlGaSb are from Ferrini et al. [4], the constants from InP come from Palik [5], the constants for AlGaAs come from Aspnes et al. [6], and the constants for Ag come from Johnson & Christy [7]. The refractive index data for AlGaAs did not reach the longer wavelengths past about 830 nm (the band gap of $Al_{0.2}Ga_{0.8}As$ is at about 700 nm), so we simply used a Lorentzian fit to the 730-830 nm tail of the real part of the index to extrapolate the refractive index.

References

(1) Adachi, S., *Properties of Semiconductor Alloys: Group-IV, III-V and II-VI Semiconductors*; John Wiley & Sons, Ltd.: 2009.

(2) Liu, V.; Fan, S. S4: A free electromagnetic solver for layered periodic structures. *Comput. Phys. Commun.* **2012**, *183*, 2233–2244.

(3) Cui, Y.; He, Y.; Jin, Y.; Ding, F.; Yang, L.; Ye, Y.; Zhong, S.; Lin, Y.; He, S. Plasmonic and metamaterial structures as electromagnetic absorbers. *Laser Photon. Rev.* **2014**, *8*, 495–520.

(4) Ferrini, R.; Patrini, M.; Franchi, S. Optical functions from 0.02 to 6 eV of $Al_xGa_{1-x}Sb$/GaSb epitaxial layers. *J. Appl. Phys.* **1998**, *84*.

(5) Palik, E., *Handbook of Optical Constants of Solids*; Elsevier Academic Press: Waltham, MA: 1985, pp 429–443.

(6) Aspnes, D. E.; Kelso, S. M.; Logan, R. A.; Bhat, R. Optical properties of $Al_xGa_{1-x}As$. *J. Appl. Phys.* **1986**, *60*, 754–767.

(7) Johnson, P. B.; Christy, R. W. Optical Constants of the Noble Metals. *Phys. Rev. B* **1972**, *6*, 4370–4379.